Development of Coastal Ocean Modeling System around Japan for Fisheries Science with the ROMS

Hiroshi Kuroda, Takashi Setou, Manabu Shimizu, Tomowo Watanabe

Fisheries Research Agency, National Research Institute of Fisheries Science,
MEDIA, Model Experimental Research Group. Contact: kurocan@affrc.go.jp

1. Introduction

We have started the development of a coastal ocean modeling system around Japan based on ROMS. The main objective is to study fish stock and recruitment variations and to help its management. The coastal waters in Japan are strongly affected by the offshore mesoscale activity from the Kuroshio and Oyashio boundary currents in the North Pacific and the Tsushima Warm Current system in Japan Sea. In addition, it has been considered that the Kuroshio Extension and Mixed Water Region east of Japan play important roles in recruitment of many fish species, such as sardine, anchovy, mackerel. As the first step for our purpose, it is thus essential to develop the eddy-resolving ocean model around Japan.

2. Model Description

2.1. Resolution and one-way nesting

Two models with low and high resolution are developed and connected by an one-way nesting technique. The parent model resolution is constant, 1/2 degree for both the zonal and meridional directions. Because of the limitation of our computational resource, the grid sizes of 1/10 and 1/6 degree are combined for the child model using the two nest ratios of 3 with 5. However, it has been reported in ROMS Discussion that such a drastic change of the model resolution is not desirable for ROMS numerics. Moreover, at this stage, the vertical resolution is 21 levels for the two models, which seem to tend to weaken the horizontal density gradient of mesoscale eddies. Therefore, as soon as sufficient computational resources can be retained, we will give the child model a constant 1/10-degree grid size and increase the vertical resolution (40~60 levels) of the two models.

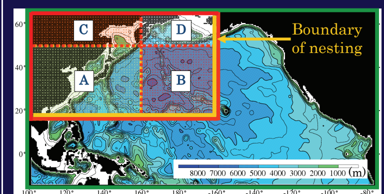

Figure 1: Topography of the parent model. Green and red squares denote the parent and child model domains, respectively. The child-model grid size (longitude by latitude) is 1/10˚ by 1/10˚ for the region of A, 1/6˚ by 1/10˚ for B,1/10˚ by 1/6˚ for C, and 1/6˚ by 1/6˚ for D. The nesting boundary is imposed on orange region.

2.2. Forcing

Spin-up experiments are performed. The two models are forced by monthly mean heat and momentum fluxes at the sea surface derived from GHRSST and JRA-25 meteorological reanalysis products (Onogi *et al.*, 2007) during the years of 1986-2006. The bulk formula based on COARE version 3 is applied for estimating the sea surface fluxes. Temperature and salinity at all vertical grid points are restored to WOA2001's monthly climatology with a time scale of 40 days near the southern and western boundaries in the parent model, and Okhotsk and Bering Seas in the two models, where sea ice is formed in winter but not explicitly computed.

2.3. Time schedule of spin-up process

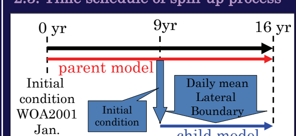

Figure 2 (left): The parent model is run for 16 years from an initial condition based on WOA2001's temperature and salinity in January (zero momentum). The child model is integrated for 8 years using an initial condition based on the 9th year output on January 1 and the daily mean lateral boundary condition estimated from the parent model.

2.4. Horizontal viscosity and diffusivity

Harmonic viscosity and diffusion are used. Large nonlinear viscosity based on Smagorinsky (1967) and non-zero background viscosity are adapted for the child model to suppress an unrealistic fluctuation of the Kuroshio path (e.g, Fig. 5(b)). It should be born in mind that the horizontal viscosity parameterization is one of the most important tuning points.

Table 1: Horizontal diffusion and viscosity parameterization

	diffusion (constant)		viscosity		
			Smagorisky	Background	
Parent model	100m/s^2	MIX_ISO	0.2	0m/s^2	MIX_S
Child model	5 m/s^2	MIX_GEO	0.3	0.1/12*grdscl m/s^2 (ROMS Default)	MIX_S

3. Results ~child model~

3.1. Mean sea surface height

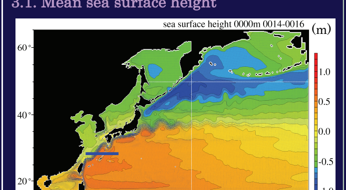

Figure 3: Mean sea surface height (contour) and sea surface current (blue vectors) in the child model averaged over 14-16th years.

GOOD POINTS

The realistic path of the Kuroshio south of Japan (nearshore non-Large meander path)

The realistic Kuroshio Extension along 35 ˚N (the 1st and 2nd troughs and crests)

WORSE POINTS

The Oyashio first branch intrusion stronger than the observation
➔Main cause is not specified

Northward overshoot of the East Korean Warm Current ➔ probably due to low vertical resolution and high horizontal viscosity

3.2. Sea surface height variability

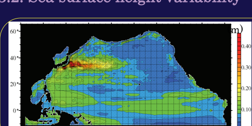

OBSERVATION

Figure 4 (left): Standard deviation of sea surface height from AVISO MADT products (1993-2006).

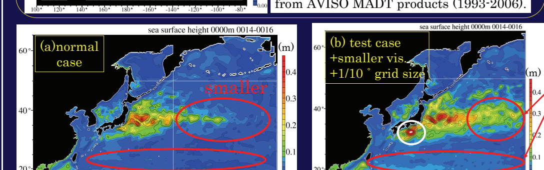

Modified

But…

Unrealistically, the Kuroshio path fluctuates south of Japan.

Figure 5: Standard deviation of sea surface height based on monthly means in the 14th-16th years. (a) normal case and (b) test case with a weaker viscosity and increased resolution (background viscosity= 0, Smagorinsky=0.2, 1/10˚×1/10˚ east of 160 ˚ E).

3.3. Volume transport

The Kuroshio transport in Tokara Strait is comparable to a few observations. Ryukyu current is simulated although its transport is somewhat smaller probably due to the high background viscosity (Table 1). The Oyashio return flow offshore the first branch is much weaker.

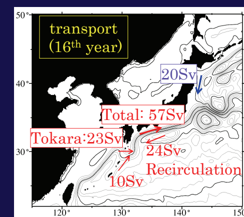

Figure 6 (left): Vertically integrated stream function estimated from 16th year output. Contour intervals are 5 and 20 Sv, denoted by thin and thick lines, respectively.

3.4. Ryukyu Current

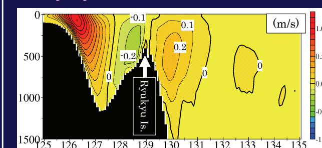

West of Ryukyu Islands
➔Surface-intensified Kuroshio
➔Kuroshio return flow (~20cm/s)

East of Ryukyu Islands
➔Ryukyu Current with an intermediate current core (200~700m)

Figure 7 (upper): Zonal section of the northeast velocity component along 28 ˚N (on the blue line in Fig. 3).

3.5. Transport through straits in Japan Sea

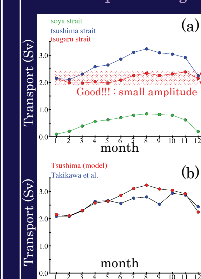

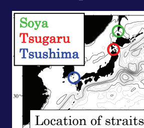

Tsushima: comparable
Soya: underestimate (0~0.3Sv)
Tsugaru: overestimate (0~0.3Sv)

Figure 8 (left):
(a) Monthly mean volume transport in major three straits of Japan Sea based on 16th year model output.
(b) Model transport in Tsushima Strait is compared with the climatology by Takikawa *et al.* (2005).

3.6. Detachment process of warm core rings

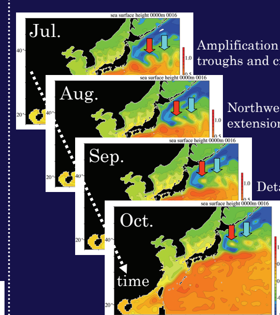

Amplification of troughs and crests

Northwestward extension of crests

Detachment

Westward propagation

Figure 9 (upper): Monthly mean sea surface height based on 16th year output of the child model.

3.7. Winter mixed layer depth

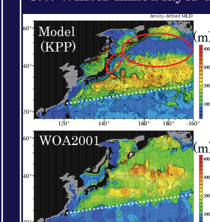

Good
100-m contour in the subtropical region

Underestimate(>50m)
the subarctic region the Oyashio region

Figure 10 (left): Max. depth of winter mixed layer based on monthly mean density in Feb. and Mar..

3.8. Annual mean temperature at 100m

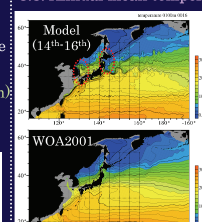

Faults
Low temperature due to the intense southward intrusion of the Oyashio

High temperature due to the overshoot of the EKWC

Figure 11 (left): Annual mean 100-m temperature .

3.9. Seasonal variation of Changjiang Diluted Water (CDW)

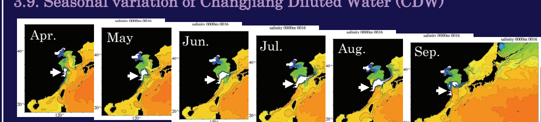

Monthly mean fresh water flux out of Changjiang River is taken account of in the child model.

Figure 12 (upper): Monthly mean sea surface salinity based on 16th year model output.

4. Problems

(1) Unrealistically intense southward intrusion of the Oyashio First Branch

(2) Shallow winter mixed layer in the subarctic and Oyashio region

(3) Overshoot of the East Korean Warm Current

(4) Failure to reproduce the bimodality of the Kuroshio path (now single mode)

The main causes of (1) and (2) have not been specified, so please give us any comments!!!

The (3) and (4) should be solved by tuning the horizontal viscosity parameterization.

5. Future works

In addition to tunings of the parent and child models, we have started to develop a triply nested coastal ocean model southwest of Japan, where the 1/10-degree model can successfully simulate the realistic Kuroshio path. The grid size of the coastal model is 1/50 degree, enough fine to well resolve topographically-induced Kuroshio frontal variability over the slope.

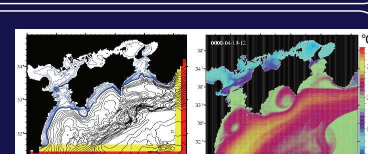

Figure 13: 1/50-degree coastal model topography (left) and snapshot of model SST (right)

Acknowledgements

Computations in the present study were carried out on a NEC SX-8 (now SX-9) multi-vector processor system and a SGI Altix 3700 cluster system at the Computer Center for Agriculture, Forestry and Fisheries Research, MAFF, Tsukuba, in Japan.